SINTEF
PROCEEDINGS
2

Proceedings of the 12th International Conference on Computational Fluid Dynamics in the Oil & Gas, Metallurgical and Process Industries

Progress in Applied CFD – CFD2017

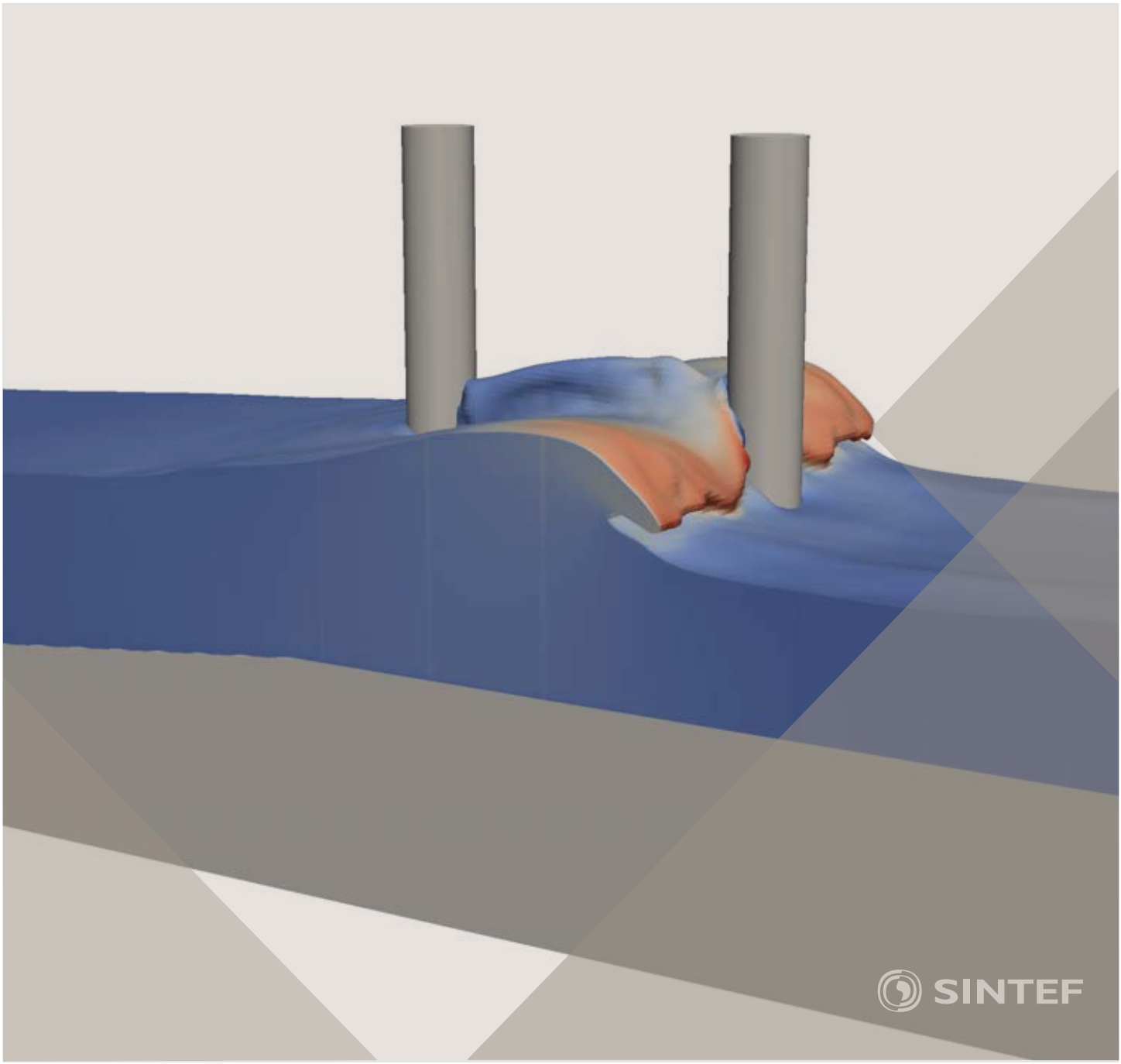

SINTEF Proceedings

Editors:
Jan Erik Olsen and Stein Tore Johansen

Progress in Applied CFD – CFD2017

Proceedings of the 12th International Conference on Computational Fluid Dynamics in the Oil & Gas, Metallurgical and Process Industries

SINTEF Academic Press

SINTEF Proceedings no 2
Editors: Jan Erik Olsen and Stein Tore Johansen
Progress in Applied CFD – CFD2017
Selected papers from 10th International Conference on Computational Fluid Dynamics in the Oil & Gas, Metallurgical and Process Industries

Key words:
CFD, Flow, Modelling

Cover, illustration: Arun Kamath

ISSN 2387-4295 (online)
ISBN 978-82-536-1544-8 (pdf)

SINTEF Academic Press
Address: Forskningsveien 3 B
PO Box 124 Blindern
N-0314 OSLO
Tel: +47 73 59 30 00
Fax: +47 22 96 55 08

www.sintef.no/byggforsk
www.sintefbok.no

SINTEF Proceedings
SINTEF Proceedings is a serial publication for peer-reviewed conference proceedings on a variety of scientific topics.
The processes of peer-reviewing of papers published in SINTEF Proceedings are administered by the conference organizers and proceedings editors. Detailed procedures will vary according to custom and practice in each scientific community.

PREFACE

This book contains all manuscripts approved by the reviewers and the organizing committee of the 12th International Conference on Computational Fluid Dynamics in the Oil & Gas, Metallurgical and Process Industries. The conference was hosted by SINTEF in Trondheim in May/June 2017 and is also known as CFD2017 for short. The conference series was initiated by CSIRO and Phil Schwarz in 1997. So far the conference has been alternating between CSIRO in Melbourne and SINTEF in Trondheim. The conferences focuses on the application of CFD in the oil and gas industries, metal production, mineral processing, power generation, chemicals and other process industries. In addition pragmatic modelling concepts and bio-mechanical applications have become an important part of the conference. The papers in this book demonstrate the current progress in applied CFD.

The conference papers undergo a review process involving two experts. Only papers accepted by the reviewers are included in the proceedings. 108 contributions were presented at the conference together with six keynote presentations. A majority of these contributions are presented by their manuscript in this collection (a few were granted to present without an accompanying manuscript).

The organizing committee would like to thank everyone who has helped with review of manuscripts, all those who helped to promote the conference and all authors who have submitted scientific contributions. We are also grateful for the support from the conference sponsors: ANSYS, SFI Metal Production and NanoSim.

Stein Tore Johansen & Jan Erik Olsen

Organizing committee:

Conference chairman: Prof. Stein Tore Johansen
Conference coordinator: Dr. Jan Erik Olsen
Dr. Bernhard Müller
Dr.Sigrid Karstad Dahl
Dr.Shahriar Amini
Dr.Ernst Meese
Dr.Josip Zoric
Dr.Jannike Solsvik
Dr.Peter Witt

Scientific committee:

Stein Tore Johansen, SINTEF/NTNU
Bernhard Müller, NTNU
Phil Schwarz, CSIRO
Akio Tomiyama, Kobe University
Hans Kuipers, Eindhoven University of Technology
Jinghai Li, Chinese Academy of Science
Markus Braun, Ansys
Simon Lo, CD-adapco
Patrick Segers, Universiteit Gent
Jiyuan Tu, RMIT
Jos Derksen, University of Aberdeen
Dmitry Eskin, Schlumberger-Doll Research
Pär Jönsson, KTH
Stefan Pirker, Johannes Kepler University
Josip Zoric, SINTEF

CONTENTS

IMPROVED COLLISION MODELLING FOR LIQUID METAL DROPLETS IN A COPPER SLAG CLEANING PROCESS

H. Yang[1*], J. Wolters[1], P. Pischke[2], H. Soltner[1], S. Eckert[3], J. Fröhlich[4]

[1] Forschungszentrum Jülich, Central Institute for Engineering, Electronics and Analytics, 52428 Jülich, Germany

[2] RWTH Aachen University, Institute of Heat- and Mass Transfer, 52062 Aachen, Germany

[3] HZDR, Department of Magneto-Hydrodynamics, 01067 Dresden, Germany

[4] TU Dresden, Institute of Fluid Mechanics, 01067 Dresden, Germany

* E-mail: h.yang@fz-juelich.de

ABSTRACT

Collision and coalescence among liquid metal droplets in a slag cleaning process enhanced by electromagnetic stirring were numerically studied. A hybrid collision algorithm was implemented to calculate the collision probability, which overcomes the mesh-dependency problem in a pure stochastic algorithm and is adaptive to both homogeneous and in-homogeneous cases. Theoretical analyses and numerical simulations based on the Volume-of-Fluid method were carried out in order to predict the result of droplet collisions, which are important for the copper slag cleaning process.. Based on the numerical results, a new regime map, which is specific to the liquid metal droplet collisions driven by shear slag flow at low capillary numbers, is provided.

Keywords: copper slag cleaning, coalescence, volume-of-fluid method, liquid metal droplet

NOMENCLATURE

Greek Symbols

ρ Mass density, [kg/m^3].
μ Dynamic viscosity, [kg/m.s].
υ Kinematic viscosity, [m^2/s].
σ Surface tension, [N/m].
$\dot{\gamma}$ Shear rate, [1/s].
λ Viscosity ratio, [-].
λ_r Size ratio, [-].
ψ Offset ratio, [-].
χ Mesh size, [m].
α Volume fraction, [-].
κ Curvature, [-].
Θ Angular velocity, [rad/s].
Γ Strain tensor, [-].
ξ Dimensionless distance, [-].
φ Angle, [rad].

Latin Symbols

p Pressure, [Pa].
$\boldsymbol{U}$ Velocity, [m/s].
t Time, [s].
$\boldsymbol{g}$ Gravitational acceleration, [m/s^2].
$\boldsymbol{J}$ Current density, [A/m^2].
$\boldsymbol{B}$ Magnetic flux density, [T].
$\boldsymbol{F}$ Force, [N].
h Distance, [m].
R Radius, [m].
V Volume, [m^3].
$\boldsymbol{n}$ Surface normal vector, [-].
$\boldsymbol{r}$ Distance vector, [-].
A_0 Hamaker constant, [J].
S_r Shape ratio [-].

Sub/superscripts

$'$ Dimensionless
d Droplet.
f Fluid.
0 Initial value or external field.
c Critical value.
i Index *i*.

INTRODUCTION

The recovery of valuable metallic material from industrial waste attracted increasing attention in past decades. In the copper production industry, slags from submerged arc furnaces (SAF) still contain up to 0.8 % of copper concentrate (Schlesinger and King, 2011). Single SAF furnaces generally produce 700,000 tons of slag per year, which represents a great economic recovery potential of the valuable copper material. As a result, a recovery furnace is conventionally arranged to recycle the remaining copper material from the SAF slag (cf. Figure 1), which allows gravitational settling of copper material onto the matte layer due to the density difference. In the slag, two thirds of the total copper is present in the form of entrained matte droplets with radii between 1 and 1000 μm (Warczok and Riveros, 2003) whereas the rest is dissolved in the slag or matte as Cu^+ ions bonded to O^{2-} or S^{2-}. A strong direct current (DC) is applied between the slag at the top and the matte layer at the bottom. The electric current generates Joule heat to keep the slag molten and to reduce the level of dissolved copper in the form of Cu_2O through electrode reactions, which segregate the dissolved copper near the anode. The segregated copper aggregates into fine dispersed droplets of 3 to 50 μm diameter (Degel, et al., 2008). Considering the droplets with small size, the gravitational settling is too slow for an efficient cleaning

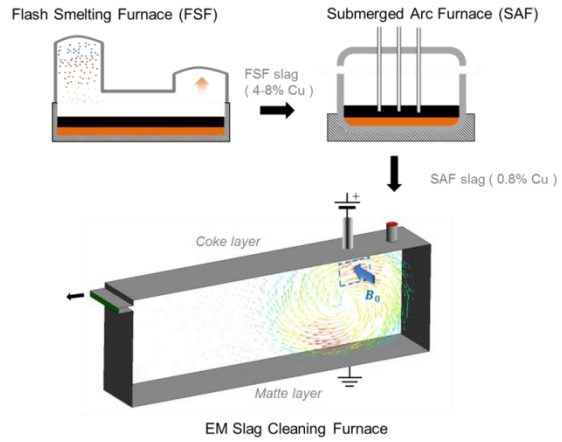

Figure 1: Flow diagram of an industrial copper production and slag cleaning process.

process. To increase the separation rate a magnetic field orthogonal to the electric field is introduced, which generates an intense stirring of the slag. Due to the stirring the probability of inter-droplet collisions is increased, which accelerates the droplet growth and results in a higher settling velocity.

In the recent years the feasibility and efficiency of the electromagnetic (EM) copper slag cleaning process has been tested experimentally at both laboratory and pilot scale (Kempken, et al., 2006). A few numerical investigations have also been published (Warczok and Riveros, 2007), which focused on predicting the dynamic and thermal behaviour of the slag phase. The inter-droplet collision and coalescence of the liquid metal droplets in molten slags, however, have not been numerically analysed despite of their dominating importance in the recovery process. Our project aims at advancing the understanding of the complex physical-chemical mechanisms in the copper slag cleaning process and optimizing the industrial process based on CFD calculations. Current numerical work is carried out using the commercial code ANSYS FLUENT.

The main focus of this paper is on analysing and modelling the outcome of binary collisions of liquid metal droplets in slags. Other numerical methods necessary to model the whole slag cleaning process, such as MHD (magneto-hydrodynamics) to simulate the forced stirring motion of the conducting slag and methods to determine the collision probability of droplets, will be mentioned but not discussed in detail.

NUMERICAL MODELS

Numerical scheme and governing equations

Our numerical investigations include multiphase modelling on the EM copper slag cleaning process, where the conducting slag is defined as the primary phase and entrained liquid metal droplets are defined as the dispersed secondary phase. The secondary phase features a small volume fraction but a massive number of droplets. Thus the current simulations are performed under an Euler–Lagrangian scheme, where the primary phase is treated as continuous phase and the secondary phase is treated as discrete phase.

For the continuous phase, the laminar flow of the conducting slag is driven and stirred by the Lorentz force. The Navier-Stokes equation for an incompressible conducting fluid under the influence of an external electromagnetic field can be expressed as:

$$\rho_f \left[\frac{\partial \boldsymbol{U}}{\partial t} + (\boldsymbol{U}\cdot\nabla)\boldsymbol{U}\right] = -\nabla P + \rho_f \boldsymbol{g} + \mu_f \nabla^2 \boldsymbol{U} + \boldsymbol{J_0}\times\boldsymbol{B_0}. \quad (1)$$

The term $\boldsymbol{J_0}\times\boldsymbol{B_0}$ is the Lorentz force density, which neglects the induction fields as the superposed field $\boldsymbol{J_0}$ and $\boldsymbol{B_0}$ are much stronger in comparison.

For the dispersed phase, the trajectory of the discrete droplet is predicted by solving the force balance equation:

$$m_d \frac{d\mathbf{U_d}}{dt} = \mathbf{F_B} + \mathbf{F_D} + \mathbf{F_{VM}} + \mathbf{F_L} + \mathbf{F_{EC}}. \quad (2)$$

Where $\boldsymbol{F_B}$ is the buoyancy force, $\boldsymbol{F_D}$ is the drag force, $\boldsymbol{F_{VM}}$ is the virtual mass force, $\boldsymbol{F_L}$ is the Lorentz force due to the higher conductivity of droplet and $\boldsymbol{F_{EC}}$ is the electro-capillary force. More details on expressions of those forces can be found in (Warczok and Riveros, 2007) and (Choo and Toguri, 1992).

Algorithm of collision probability calculation

In the present application, the direct modelling of collisions for all single droplets is prohibitive, since their large number would lead to unacceptable computational costs. This is avoided by a stochastic modelling, where the concept of parcels, representing a certain number of droplets with the same properties, is introduced. The most commonly used algorithm for collision modelling is a pure stochastic Monte Carlo algorithm, which is based on concepts of the kinetic gas theory (O'Rourke, 1981). It assumes that the droplets are homogeneously distributed in the collision volume. The collision probability depends on the mesh resolution, because the collision between droplets of two parcels is only possible when the centres of both parcels are located in the same cell of the continuous phase. The result of the pure stochastic algorithm highly depends on the spatial resolution and the error can become significant for cases with relatively coarse grids. The accuracy of this algorithm could be increased to second order through refining the control volume mesh. However, it may be computationally very costly to introduce such a refinement in geometrically complex simulations and it is difficult to estimate the appropriate mesh-resolution for different cases in advance. To overcome mesh dependency problems in the pure stochastic collision algorithm, a new hybrid Lagrangian collision algorithm was proposed by Pischke (2012). Here, the deterministic algorithm is transferred into a stochastic algorithm by redefining the number of collisions assuming a normal probability of presence of droplets around the centres of the parcels. The hybrid algorithm is absolutely mesh-independent and third-order accuracy can be achieved for inhomogeneous cases. Due to this advantage, the hybrid algorithm was chosen and implemented for the present simulations. In our former work (Yang, et al., 2016) we have investigated the differences between the two algorithms in detail.

Prediction on collision outcome

To predict the collision outcome in a stochastic collision modelling, a regime map, which normally uses two or more parameters to identify the boundary among different possible collision outcomes, is required. Ready-to-use regime maps, such as suggested by Qian and Law (1997), are typically based on inertia-driven collisions in a gas-liquid-system with the Weber number (We) as the main criterion. Those regime maps, however, are physically not suitable for our liquid metal droplet-slag system as stated in the following.

First of all the collision process of droplets in our system features very small Weber numbers, which would lead to droplet coalescence under the inertia-driven scheme. Instead of using criterion of an inertia-driven collision, it is physically more suitable to use the capillary number as the main criterion, which includes the influencing factors of shear-driven collisions like in our case.

Moreover, if the surfactant effect is neglected, collisions can be classified by the viscosity ratio between the droplet and fluid phase (Abid and Chesters, 1994). The outcome of a binary collision is determined by the drainage process of the thin film of the surrounding fluid trapped between confronting surfaces of the colliding droplets. The flow in the film can be described by the profile shown in Figure 2, depending on the viscosity ratio λ. When $\lambda \gg 1$, the interfaces are immobile and a Poiseuille flow type can be used to describe the drainage process. This is also the case for most of the Weber number based regime maps, where liquid droplets in gaseous environment are studied. When $\lambda \sim 0$, the film interfaces are fully mobile and the film drainage can be described as a plug flow. When λ has a moderate value, such as in our case for the liquid metal droplets-slag system, a partially mobile film interface is considered, where the drainage flow is a superposition of the Poiseuille and the plug flow. The regime maps which exclude such an influence brought by the viscosity ratio will cause an inaccurate prediction on the collision results.

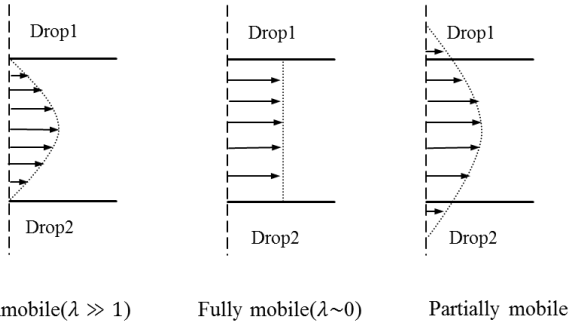

Figure 2: Classification of film drainage flow profile based on the viscosity ratio

Based on the above mentioned reasons, it is necessary to develop an appropriate outcome regime map for the liquid metal droplets-slag system. However, experimental results are difficult to achieve in such an opaque, high-temperature environment and no available experimental data have been found. Thus, in current investigations the collision process is studied theoretically and numerically to provide a suitable outcome regime map.

ANALYSIS AND MODELLING OF THE BINARY COLLISION PROCESS

For numerically solving multiphase problems on two immiscible fluids with distinct interfaces, the volume of fluid (VoF) method is appropriate and is therefore chosen to model the binary collision process of liquid metal droplets entrained in a molten slag.

Fundamental principles of a shear driven binary collision

Similar to the analysis by Mousa (2001), a binary collision process in a simple shear flow can be illustrated according to Figure 3. The droplets are assumed to have equal size ($R_1 = R_2 = R$) and droplet 2 is driven towards droplet 1 by the shear flow ($\boldsymbol{U} = \sim(\dot{\gamma}\Delta y, 0,0)$) in a straight line until they are close enough to interact with each other. At this point the confronting interfaces of the two droplets are flattened and the thin film of surrounding fluid starts to drain under the influence of hydrodynamic forces exerted by the shear flow and inter-molecular forces. If the drainage of the film is accomplished before droplets are separated by the external flow, the collision will end up in coalescence, at least temporarily. Otherwise, the droplets will slide along each other's surfaces and the collision ends up in bouncing.

The important dimensionless parameters to characterize the process are:

$$\mathrm{Ca} = \mu_f \frac{\dot{\gamma} R}{\sigma}, \qquad Re = \frac{\dot{\gamma} R^2}{\nu}, \quad \psi = \frac{\Delta y}{2R}, \quad \lambda = \frac{\mu_d}{\mu_f}$$

$$h'(t) = \frac{h(t)}{R}, t' = \dot{\gamma} t.$$

Where, $\dot{\gamma}$ is the shear rate, σ is surface tension, ν is the kinetic viscosity, μ_d and μ_f are dynamic viscosity for droplet and bulk phase.

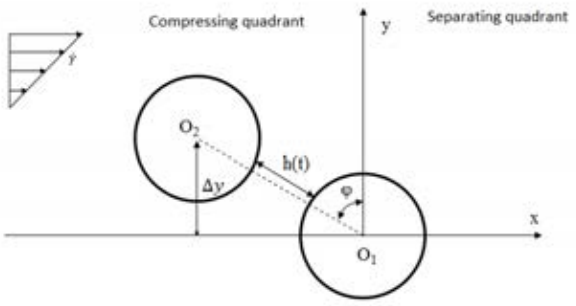

Figure 3: Sketch of a binary collision process

Basics of the VoF method and governing equations

When the VoF method is used, additional transport equations for the volume fraction of phase *i* have to be solved. Under the prerequisites that no mass transfer between different phases is allowed and no mass source exists, the transport equation for the volume fraction α_i for incompressible fluids is given by

$$\frac{\boldsymbol{D}\alpha_i}{\boldsymbol{D}t} = \frac{\partial \alpha_i}{\partial t} + (\boldsymbol{U}\cdot\nabla)\alpha_i = 0. \quad (3)$$

In order to resolve the shape of the interface between different phases, a geometric reconstruction interpolation method (Young, 1982) is applied. This highly accurate, piecewise-linear approach recalculates a linear interface in each boundary cell filled with more than one phase based on the volume fraction and the corresponding derivative. To use the interface tracking method, an explicit scheme must be applied:

$$\frac{\alpha_i^{n+1} - \alpha_i^n}{\Delta t} + \frac{\sum_f (U_f^n \alpha_{i,f}^n)}{V} = 0. \quad (4)$$

Where V is the cell volume and *f* is the subscript that indicates a face value.

Compared with the implicit scheme, where the volume fraction value from the previous time step is not needed, the explicit scheme does not iteratively solve the transport equation of the volume fraction in each time step. The numerical diffusion of the interface is as a result less significant to in the implicit scheme and the prediction on the interface curvature is more accurate.

In the VoF method the intermolecular surface tension is normally modelled by solving the continuum surface force. At interface cells the gradient of the rise in pressure due to interfacial tension between different phases can be represented as volumetric body force F_{sf} (Brackbill, et al., 1992). The force is added as a source term in the momentum equation and can be expressed as:

$$\boldsymbol{F_{sf}} = 2\cdot\alpha_1(t)\cdot\kappa(t)\cdot\boldsymbol{n}(t)\cdot\sigma. \quad (5)$$

$n(t)$ is the surface normal vector, which is defined as the gradient of the second phase volume fraction:

$$\boldsymbol{n}(t) = \nabla\alpha_1(t). \quad (6)$$

$\kappa(t)$ is the local surface curvature and can be calculated by:

$$\kappa = \frac{1}{|\boldsymbol{n}|}\left[\left(\frac{\boldsymbol{n}}{|\boldsymbol{n}|}\cdot\nabla\right)|\boldsymbol{n}| - (\nabla\cdot\boldsymbol{n})\right]. \quad (7)$$

Coalescence criterion

As mentioned before, the film drainage process is controlled by both hydrodynamic forces and inter-molecular forces, such as the Van der Waals force F_{vdw}. However, in the finite-volume modelling it is very difficult to precisely model the end of the drainage process in the case of coalescence ($h(t) = 0$). Moreover, according to detailed calculations by Jiang and James (2007), F_{vdw} is only considerably large when *h(t)* is very small. Therefore, in our calculations coalescence is detected when the critical thickness of the film h_c according to equation (8) is reached:

$$h_c = \left(\frac{AR}{8\pi\sigma}\right)^{\frac{1}{3}}. \quad (8)$$

According to the research by Chesters (1991), this approximate relationship is valid for flow-driven collisions between fluid-liquid dispersions at low capillary number. Once the critical film thickness is reached, F_{vdw} becomes significant and increases rapidly. The destabilization due to F_{vdw} dominates the film drainage, which leads to a film rupture and coalescence. This coalescence criterion was applied in several former researches, like for example in (Mousa, 2001). Mousa theoretically investigated collisions with partially and fully mobile interfaces at arbitrary approaching angles.

In our calculations, we exclude the contribution of F_{vdw}, thus the collision is purely driven by the hydrodynamic forces and coalescence is reached if *h(t)* becomes less than h_c. The value of *h(t)* is determined by the minimum distance between the iso-surfaces of two droplets defined by the volume fraction.

The critical film thickness for metallic material in comparison to polymeric material is shown in Figure 4 as a function of the droplet size. The latter is extensively studied in experiments. A typical value for the Hamaker constant A of metallic material is $40\times10^{-20}J$, while for polymeric material it is $1\times10^{-20}J$ (Chen, et al., 2009). The surface tension of copper droplets in slag is $\sim0.05\frac{N}{m}$, while for polymeric systems it is $\sim0.005\frac{N}{m}$. Thus the coalescence efficiency of copper droplets in a slag can be expected to be larger than that of polymeric material reported by Bruyn (2013).

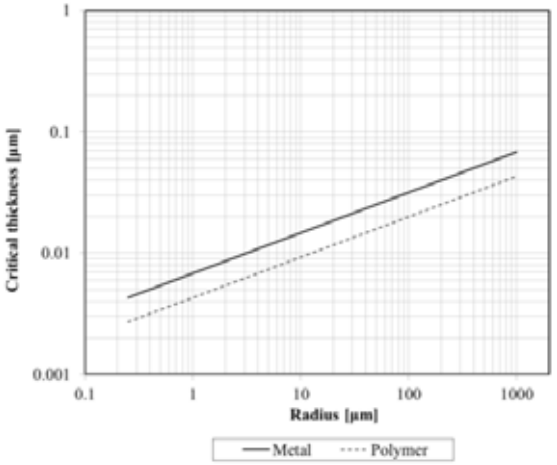

Figure 4: Critical film thickness for coalescence of metallic and polymeric material

Numerical setups

Geometry

A sketch of the 3D model to numerically simulate the binary collision process is shown in Figure 5. A simple shear flow at the desired shear rate is generated by two non-slip walls at the top and bottom of the domain, moving in opposite direction, and a periodic boundary condition. The centers of the two droplets are initially located in the middle of one symmetry plane at different y-positions, according to the demanded offset ratio. The initial distance in x-direction is fixed at $\Delta x = 2.52R$ so

that the simulations start with non-interacting droplets until their shapes adapt to the flow field. The value of Δx is chosen according to the film drainage analysis (Chesters, 1991), where the film is established at the distance $h(t) \leq 0.5\,R$. Similar to an experimental setup described by Bruyn (2013), the distance between the moving walls is *36 R* to avoid confinement effects. Periodic boundary conditions are used to ensure a fully developed shear flow. The distance between the two periodic planes is *20 R,* which is large enough to eliminate the influence due to the mirrored droplet pairs.

Mesh

The modelling of the film drainage process requires meshes near the droplets surface with high resolution. However, it is computationally too expensive to generate meshes with identical sizes for the whole domain. Therefore a centre zone of size $6R \times 6R \times 2R$ with sufficiently fine resolutions around the droplets is defined and the mesh resolution outside this zone is 10 times coarser. The boundary faces between the zone with fine and coarse mesh are defined as interfaces to allow mass and momentum transfer of the fluid. Furthermore, in the area near the droplets interface with the bulk phase, a 1-level dynamic adaption of the mesh based on the gradient of the phase volume fraction is defined.

When choosing a proper mesh resolution, several aspects have to be considered:

First of all the mesh size χ must be small enough to prevent the merging between interfaces of two droplets in the same cell before *h(t)* reaches the critical value h_c ($\chi \leq \frac{h_c}{2}$).

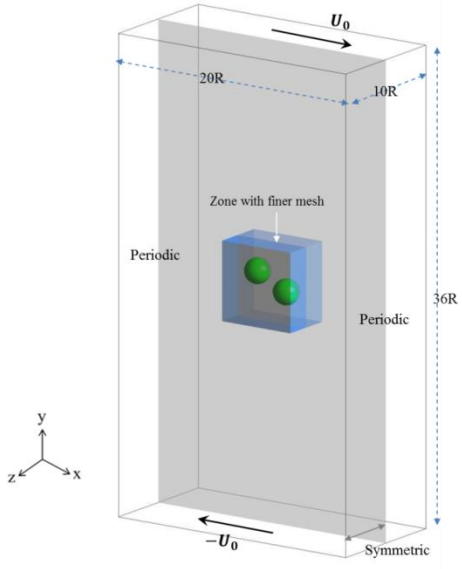

Figure 5: Geometry of the domain for modelling the binary collision

Moreover, the value of R/χ must be sufficiently large to obtain a reasonable pressure distribution inside and outside of the droplet due to the Laplace pressure between the immiscible droplet and bulk phase (Sman and Graaf, 2008):

$$\Delta p = \frac{2\sigma}{R}. \qquad (9)$$

In the VoF method, material is defined as a mixture of bulk and droplet phase in cells containing both phases, which physically do not exist. A finer mesh can reduce the error of the pressure distribution near the interface calculated with the VoF method in comparison to the theoretical value. This is important for modelling the film drainage process when interfaces of two droplets are close to each other.

On the other hand the value of R/χ cannot be increased in the VoF method without limitation. One limitation is the error due to parasitic currents (unphysical flow near the interface) (Havie, et al., 2005), which is due to the local variations of the body force calculated by the surface tension algorithm. The magnitude of parasitic current becomes stronger with a finer mesh. The influence of the parasitic current is less significant in shear driven flows. But it will still cause diverging solutions on interface tracking when the magnitude of the parasitic current is too strong in comparison with the local external flow field.

Considering the above mentioned aspects and limitations due to the available computer cluster, the mesh resolution of studied cases is chosen as:

$$h_c = 2\,\chi, R = 126\,\chi.$$

According to the relationship between h_c and R in Figure 4, the physical size of the modelled droplets is $R = 0.284\ \mu m$.

Time step

The time step in an explicit VoF calculation must be small enough to ensure a stable iteration. In practice, the global Courant number should be smaller than 2. But in cases where a more accurate interface calculation is needed, it is preferred to choose a global Courant number smaller than 1. In the current calculations, the time steps are on the order of $10\ ns$ leading to a maximum Courant number in the order of $O(10^{-1})$.

Comparison of the time evolution of the film thickness from VoF calculations and far-field trajectory analyses

The binary collision between Newtonian droplets has been widely studied theoretically. At the present stage a trajectory analysis suggested in (Wang, et al., 1994) is used to verify the accuracy of the results from VoF calculations. This method assumes that two viscous droplets are approaching each other in a simple shear flow at a small capillary number and the shapes of droplets remain nearly spherical. Meanwhile the droplets are rotating at a constant angular velocity. The relative velocity of droplet 1 moving towards droplet 2 can be determined by:

$$\boldsymbol{V_{12}}(\boldsymbol{r}) = \boldsymbol{\Theta} \times \mathbf{r} + \boldsymbol{\Gamma} \cdot \mathbf{r} - \left[\frac{\mathrm{A}(\xi)\mathbf{rr}}{\mathrm{r}^2} + \mathrm{B}(\xi)\left(\boldsymbol{I} - \frac{\boldsymbol{rr}}{r^2}\right)\right] \cdot \boldsymbol{\Gamma} \cdot \mathbf{r}. \qquad (10)$$

Where **r** is the direction vector between the two droplet centers O_1 and O_2, **I** is the unit second tensor, **Θ** is the angular velocity of the rotating droplet and **Γ** is the strain tensor of the linear shear flow. $\xi = h'(t) + 2$, $A(\xi)$ and $B(\xi)$ are relative mobility functions with respect of the viscosity ratio.

Due to the complexity of the flow situation when droplets are close to each other, the far-field expressions suggested in (Wang, et al., 1994) for the mobility functions are firstly considered:

$$A(\xi) = 4\frac{(2+5\lambda)}{(1+\lambda)}\frac{1}{\xi^3} - 48\frac{\lambda(2+\lambda)+\lambda(2+5\lambda)}{(1+\lambda)(2+3\lambda)}\frac{1}{\xi^5} + O\left(\frac{1}{\xi^8}\right), \quad (11)$$

$$B(\xi) = 32\frac{\lambda(2+3\lambda)+\lambda(2+5\lambda)}{(1+\lambda)(2+3\lambda)}\frac{1}{\xi^5} + O\left(\frac{1}{\xi^6}\right). \quad (12)$$

The dimensionless trajectory equations are thereby given as:

$$\frac{d\xi}{dt'} = -\left(1 - A(\xi)\right)\xi\sin(2\alpha), \quad (13)$$

$$\frac{d\alpha}{dt'} = -\cos^2\alpha - 0.5\,B(\xi)(\sin^2\alpha - \cos^2\alpha). \quad (14)$$

The set of differential equations (13) and (14) is numerically solved by a fifth-order Runge-Kutta method. However, the expressions for the mobility functions given in (11) and (12) are only accurate when the dimensionless distance $h(t)'$ is larger than ~0.1. To characterize the shape deformation of the droplets in a shear flow, a shape ratio S_r is defined as the ratio between the short axis length and the long axis length.

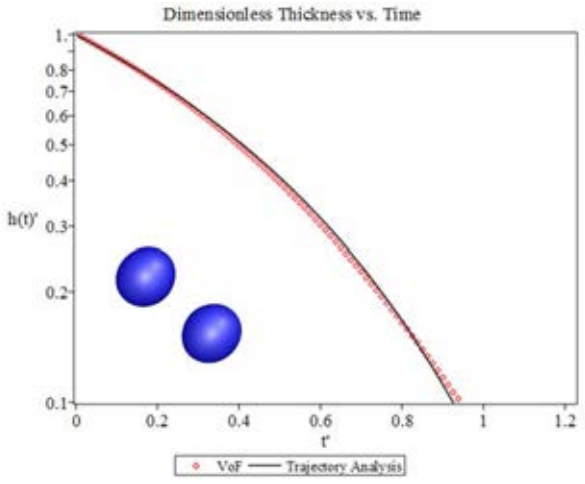

Figure 6: Time evolution of dimensionless distance between droplets' surfaces with VoF calculation and trajectory analysis ($Ca = 0.05, \psi = 0.95, S_r = 0.9$)

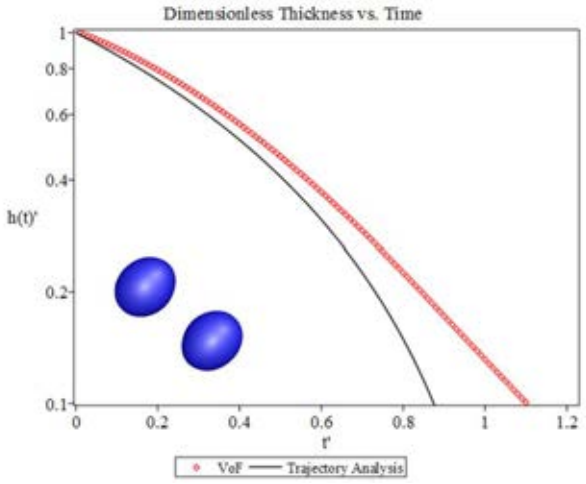

Figure 7: Time evolution of dimensionless distance between droplets' surfaces with VoF calculation and trajectory analysis ($Ca = 0.1, \psi = 0.9, S_r = 0.8$)

Binary collision test cases with $\mathrm{Ca} = 0.05$, $\psi = 0.95$, $S_r = 0.9$ and $\mathrm{Ca} = 0.1$, $\psi = 0.9$, $S_r = 0.8$ are used to compare the time evolutions of $h(t)'$ solved by the trajectory analysis and VoF calculations up to a dimensionless distance $h(t)' = 0.1$. The tracking of film thickness starts at $h(t)' = 1$, which is shown in Figure 6 and Figure 7. Shapes of droplets at $t' = 0$ are also shown in these figures. The given shape ratio S_r is due to the shear flow while the two droplets approach each other but do not yet interact. At low capillary numbers the deformation of the droplets does not affect the approaching process significantly and at large distances the results of the trajectory analysis and the VoF calculation agree well with each other (Figure 6). At larger capillary numbers the deformation of the droplets is more significant and the trajectory analysis for spherical droplets will overestimate the approaching speed (Figure 7).

Collision outcome regime map of liquid metal droplets in a slag based on VoF calculations

As it was discussed before, in a simple shear flow at low capillary numbers the possible outcome after a binary collision is coalescence or bouncing (cf. Figure 8). To determine the critical offset ratio that separates the areas of coalescence and bouncing in an outcome regime map, for different capillary numbers a series of simulations were carried out approach the critical offset ratio ψ up to an accuracy of 2 decimal places by a bisection method. Coalescence is always considered permanent when the critical film thickness is reached, because according to (Shardt, 2013) a temporary bridge (temporary coalescence with subsequent separation) between droplets is only possible when $R/h_c < 22$. In our case this would mean that the corresponding droplets must have a very small physical size of $R < 50$ nm, while the smallest droplets existing in the copper slag cleaning process have a size in the order of 1 µm.

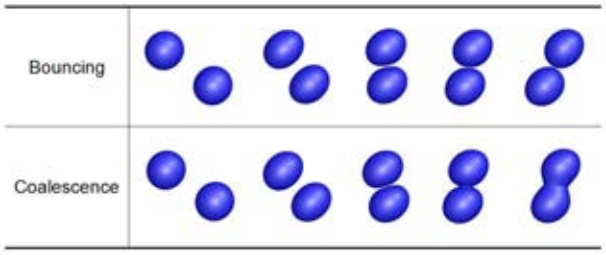

Figure 8: Possible collision outcomes in the VoF calculations

In Figure 9 the drainage process of the thin film and its possible outcome depending on the offset ratio is exemplarily shown for two different capillary numbers. In the VoF calculations, where the deformation of the droplets is balanced by the ambient pressure and surface tension, the droplets will gradually restore their shape after they pass the compressing quadrant ($\varphi > 0,\ cf. Figure\ 3$). The confronting faces of the droplets will still be pushed towards each other by the surface tension, although the hydrodynamic force tends to separate them. Therefore coalescence between droplets is still possible even if they are located in the separating quadrant of Figure 3 (cf. point $\varphi = 0$ for curve 1 in Figure 9.). It should be noted that for the assessment of the collision process and the final regime map the previously defined capillary number is multiplied by an empirical factor $\left(\frac{R}{\mu m}\right)^{0.84}$, which reflects the influence due to the physical size of the droplets to the coalescence efficiency and will be discussed in the following section.

In a regime map where $Ca \cdot \left(\frac{R}{\mu m}\right)^{0.84}$ is defined as x-axis and ψ is defined as y-axis, the curve of critical offset ratio that separates the zones of bouncing and coalescence is drawn by a polynomial interpolation (cf. Figure 10).

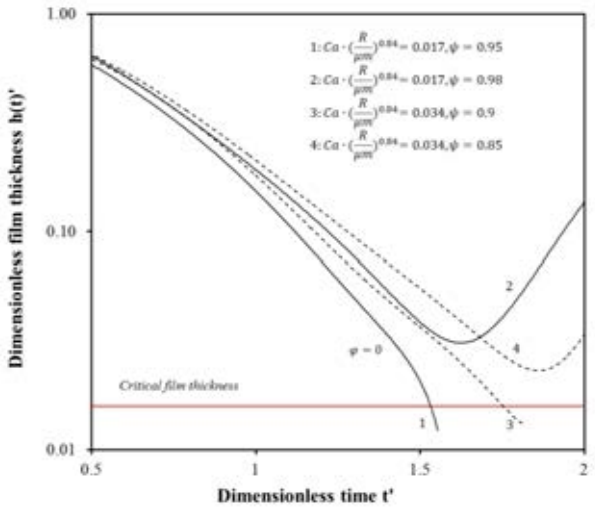

Figure 9: h(t)' versus t' for cases with different modified capillary number and offset ratio.

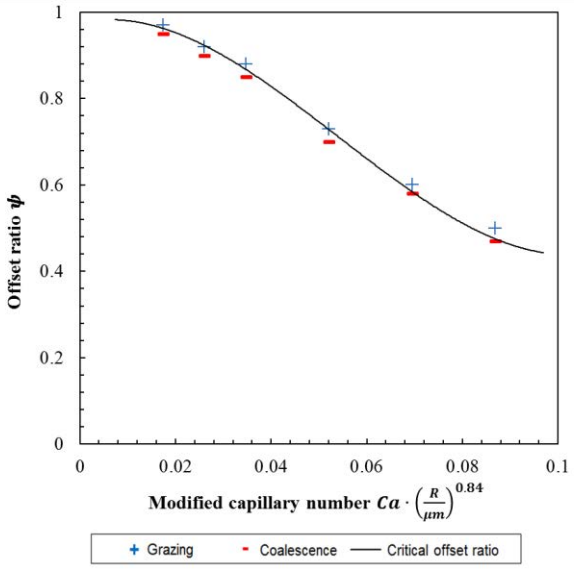

Figure 10: A capillary-number-based collision outcome regime map

DISCUSSION

When the dielectric properties of the studied collision system are constant, the regime map suggested in Figure 10 depends on the following chosen physical parameters: the physical size of the droplets, the size ratio and the viscosity ratio. Their influence will be shortly discussed in the following.

Physical size of the droplets

Instead of the pure capillary number *Ca*, a scaled number $Ca \cdot \left(\frac{R}{\mu m}\right)^{0.84}$ is used in the regime map. The scaling factor is an empirical factor resulting from experiments described in (Hu, et al., 1989) and has been used to fit experimental data (Bruyn, et al., 2013). It indicates that for larger droplets the film drainage is slower than for smaller droplets if the same capillary number is considered. The numerical approach to examine the decrease in coalescence with a larger droplet size, however, is found to be difficult (Yoon, et al., 2007). In the corresponding simulations the decrease in coalescence efficiency is mainly due to the difference in the critical thickness calculated by equation (**8**) and the dependency of the dimensionless film drainage time on the droplet size is much weaker than that observed in the experiment. The possible reasons for this disagreement have been briefly discussed in the same literature. To avoid extra simulations with different droplet sizes, which will probably fail to provide a reliable correction factor, the modified capillary number $Ca \cdot R^{0.84}$ is used currently to eliminate the effect of droplet size.

Size ratio

The size ratio of two colliding droplets is defined as $\lambda_r = \mathrm{R_{smaller}}/\mathrm{R_{larger}}$ and current investigations were under the assumption that two colliding droplets have an equal size ($\lambda_r = 1$). Theoretical analyses (Wang, et al., 1994) and experimental observations (Mousa, et al., 2001) show that for a constant average radius the coalescence efficiency decreases if the difference in size increases ($\lambda_r < 1$). This decrease in coalescence efficiency is due to the fact that smaller droplets tend to

follow the flow streamline bent around the larger droplet in the Stokes regime. The decreasing factor suggested by Mousa (1991) can be expressed as $\left(\frac{4\lambda_r}{(1+\lambda_r)^2}\right)^{\kappa}$, where κ is an empirical parameter, normally in the range from 1 to 6.

Viscosity ratio

Based on the analyses in the former section it is clear that the viscosity ratio λ, which determines the mobility of the interfaces, has a great influence on the collision result. A simple power-law dependence of coalescence on λ was expected in some early investigations, for example, in the research by Hu (1989), a relationship of $Ca_c \sim \lambda^{-2/3}$ using simple scaling theory is suggested, where Ca_c is the critical capillary number of coalescence for collision at fixed offset ratio. However, more recent researches (Yoon, et al., 2005) suggest that the influence on coalescence efficiency due to λ is more complex and it is not suitable to define a simple power-law dependency between those two parameters. To numerically investigate the influence due to the viscosity ratio simulations using the above mentioned setups with different λ were performed. The change of the critical offset ratios in the regime map based on the VoF simulations is shown in Figure 11. It can be seen that the influence of the viscosity ratio λ is more significant at higher capillary numbers. More investigations on this issue may be necessary. For the simulations on the copper slag cleaning process the influence of the viscosity ratio is important, since the temperature distribution in the slag is inhomogeneous and the viscosity ratio depends on the temperature.

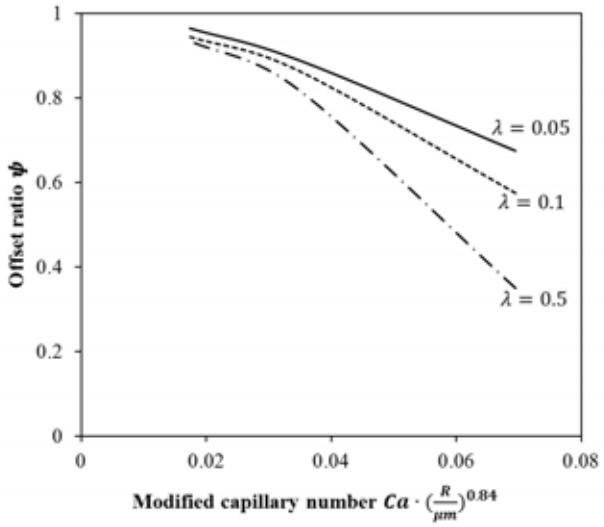

Figure 11: Critical offset ratio with respect of different viscosity ratios in the VoF calculations.

CONCLUSIONS

Numerical approaches on modelling an enhanced copper slag cleaning process through electromagnetic stirring have been presented in this publication. An Euler-Lagrangian scheme of solving the multiphase problem is implemented, where slags are defined as continuous phase and liquid metal droplets are defined as dispersed phase. For the continuous phase, MHD (magneto-hydrodynamic) calculations on the conducting slags under the influence of orthogonally oriented magnetic and electric fields were performed. For the dispersed phase tracking of the liquid metal droplet is realized by solving the force balance with consideration of special electromagnetic forces.

With respect to the inter-droplet collisions, a mesh-independent hybrid Lagrange-stochastic collision algorithm was introduced to calculate the collision probability, which has an excellent adaptability in both homogenous and in-homogenous cases.

In order to correctly predict the collision outcome in the stochastic collision modelling, a new outcome regime map was developed, taking into account the peculiarities of the slag cleaning process and physical properties of liquid metal droplets in slags. Since the collision of droplets in the slag is not driven by inertia effects but by a shear flow, the new regime map is based on the capillary number. The criteria for coalescence were derived by detailed numerical simulations on the binary collision of droplets in a slag using the Volume of Fluid (VoF) method, considering theoretical aspects and empirical findings. Intermolecular forces are not directly considered in the numerical simulation, but they determine the critical thickness of the film between the colliding droplets, for which coalescence is expected. The accuracy of the VoF calculation is verified by comparison with results from the far-field trajectory analysis. The influences due to some parameters, like droplet size, size ratio and viscosity ratio, are discussed and will also be considered in the application of the regime map.

The new regime map predicting the collision outcome in the stochastic collision model will be used in the overall copper slag cleaning process simulations. Based on these simulations an optimization of the process resulting in an improved recovery rate is envisaged in the near future.

REFERENCES

ABID, S. and CHESTERS, A.K., (1994), The drainage and rupture of partially mobile films between colliding drops at constant approach velocity, *Int. J. Multiphase. Flow,* Vol.20, No.3: 613-629.

BRACKBILL, J. U., KOTHE, D. B., ZEMACH, C., (1992), A continuum method for modeling surface tension". *J.Comput. Phys*. 100. 335–354.

BRUYN, P. D., CARDINAELS, R., MOLDENAERS, P., (2013), The effect of geometrical confinement on coalescence efficiency of droplet pairs in shear flow, *J. Colloid Interface Sci*. 409,183−192.

CHESTERS, A., (1991), The modelling of coalescence processes in fluid-liquid dispersions, *Trans. IChemE*, 69, pp. 259-270.

CHEN, D., CARDINAELS, R., MOLDENAERS, P., (2009), Effect of confinement on droplet coalescence in shear flow, *Langmuir*, 25(22): 12885-12893.

CHOO, R.T.C. and TOGURI, J.M., (1992), The electrodynamic behavior of metal and metal sulphide droplets in slags, *Canadian Metallurgical Quarterly*, Vol.31, No.2: 113-126.

DAVIS, R.H., SCHONBERG, J.A., RALLISON, J.M., (1989), The lubrication force between two viscous drops, *Phy. Fluids*, 1(1): 77-81.

DEGEL, R., OTERDOOM, H., KUNZE, J., WARCZOK, A., RIVEROS, G.,(2008), Latest results of the slag cleaning reactor for copper recovery and its potential for the PGM industry, *Third International Platinum Conference 'Platinum in Transformation'*: 197-202.

HARVIE, D.J.E., DAVIDSON, M.R., RUDMAN, M., (2005), An analysis of parasitic current generation in volume of fluid simulations, *ANZIAM J.*46: ppC133-C146.

HU, Y.T., PINE, D.J., LEAL, L.G., (1989), Drop deformation, breakup, and coalescence with compatibilizer. *Phys. Fluids*, 12: 484-489.

JIANG, X. and JAMES, J., (2007), Numerical simulation of the head-on collision of two equal-sized drops with van der Waals force, *J. Eng. Math*. 59: 99-121.

KEMPKEN, J., DEGEL, R., SCHREITER, T., SCHMIEDEN, H., Rectangular furnace design and revolutionary DC-Slag cleaning technology for the PGM industry. (2006), *Metal world,* issue 12*: 10-13*.

MOUSA, H., AGTEROF, W., MELLEMA, J., (2001), Experimental investigation of the orthokinetic coalescence efficiency of droplets in simple shear flow, *J. Colloid Interface Sci*. 240: 340-348.

MOUSA, H. and VAN DE VEN, T.G.M., (1991), Stability of water-in-oil emulsions in simple shear flow 1. Determination of the orthokinetic coalescence efficiency, *Colloide surface*, 60: 19-38.

MOUSA, H., AGTEROF, W., MELLEMA, J., (2001), Theoretical and experimental investigation of the coalescence efficiency of droplets in simple shear flow, *Progr Colloid Polym Sci.,* 118, pp. 208-215.

O'ROURKE, P.J., (1981), Collective drop effects on vaporizing liquid sprays, Ph.D thesis, Department of Mechanical and Aerospace Engineering, Princeton University.

PISCHKE, P., CORDES, D. , KNEER, R., (2012), A collision algorithm for anisotropic disperse flows based on ellipsoidal parcel representations, *Int. J. Multiphase, Flow*, 38, pp. 1–16.

QIAN, J. and LAW, C.K., (1991), Regimes of coalescence and separation in droplet collision, *J. Fluid Mech.*, 331, pp. 59-80.

SHARDT, O., MITRA, S.K., DERKSEN, J.J., (2013), Simulations of Droplet Coalescence in Simple Shear Flow, *Langmuir*, 29, pp. 6201-6212.

WANG, H., ZINCHENKO, A., DAVIS, R., (1994), The collision rate of small drops in linear flow fields, *J. Fluid Mech.,* Vol.265: 161-188.

SCHLESINGER, M. and KING, M., (2011), *Extractive metallurgy of copper*, *5th ed.,* Elsevier, UK.

VAN DER SMAN, R.G.M. and VAN DER GRAAF, S., (2008), Emulsion droplet deformation and breakup with Lattice Boltzmann model, *Computer Physics Communications*, 178: 492-504.

WARCZOK, A. and RIVEROS, G., (2003), Effect of electric and magnetic fields on the metallic inclusions in a liquid slag, *Yazawa International Symposium-Metallurgical and materials processing and technology Volume 2:* 417-429.

WARCZOK, A. and RIVEROS, G., (2007), Slag cleaning in crossed electric and magnetic fields, *Miner.Eng.*, 20: 34-43.

YANG, H., WOLTERS, J., PISCHKE, P, Soltner, H., ECKERT, S., FRÖHLICH, J., (2016), Numerical simulations on copper droplet collisions in the slag cleaning process, *9th International Conference on Multiphase Flow,* Firenze, Italy.

YOUNGS, D. L., (1982), Time-dependent multi-material flow with large fluid distortion. *Numerical Methods for Fluid Dynamics, 24(2)*: 273-285.

YOON, Y., BORRELL, M., PARK, C.C., LEAL, L.G., (2007), Coalescence of two equal-sized deformable drops in an axisymmetric flow, *Phy. Fluids*, 19(10).

YOON, Y., BORRELL, M., PARK, C.C., LEAL, L.G., (2005), Viscosity ratio effects on the coalescence of two equal-sized drops in a two-dimensional linear flow, *J. Fluid Mech.*, vol.525: 355-379.